Check for updates

Design guidelines for chalcogenide-based flexible thermoelectric materials

Yifan Wang,[abc] Peijian Lin,[a] Qing Lou,[a] Zhongchi Zhang,[a] Shan Huang,*[abc] Yao Lu*[abc] and Jiaqing He [iD] *[abc]

The power source of rapidly developed flexible and wearable intelligent electronic devices should be stable and have a long working period. Flexible thermoelectric (TE) generators (TEGs) can continuously power electronic devices by harvesting heat from the human body and have become a feasible solution. They are an economical approach to energy collection and have other advantages including chemical stability and noiselessness. Here, we review recently reported chalcogenide-based flexible TE materials and divide them into three categories: flexible substrate supported films, organic-chalcogenide composites, and free-standing flexible films. We discuss recent breakthroughs for chalcogenide-based flexible TE materials with high power factors and/or figures of merit and provide detailed design guidelines for the TE properties and flexibility of the films. We further describe how these films may be assembled into device designs that take advantage of their mechanical flexibility and thermoelectric properties. Besides, the outlook and challenges of wearable inorganic-based thermoelectric materials are proposed.

1. Introduction

Thermoelectric (TE) materials are "green" and functional materials that can realize a direct transition between heat and electricity or *vice versa*. TE generators (TEGs) are one of the most common applications of TE materials.[1] TEGs have incomparable advantages including no noise, no moving parts, easy maintenance, long working life, and high reliability. A famous application is radio-isotope batteries used in numerous NASA missions, *e.g.*, the Voyager series.[2] Therefore, a systematic review is necessary to gain a comprehensive understanding of the development of TE materials.[3–5]

The TE effect transforms heat and electricity including the Seebeck effect and Peltier effect. The process of transforming heat into electricity is called the Seebeck effect, and the reverse is called the Peltier effect.[6] A heat gradient causes a redistribution of carriers, and a concentration gradient is built, thus leading to an electrostatic potential called Seebeck voltage.[7] The Seebeck coefficient (S) is used to describe such a phenomenon and is defined as $S = \frac{1}{e}\frac{\partial_x \mu}{\partial T}$, where e is the unit charge, μ is

the chemical potential, and T is the temperature. The TE performance is usually denoted as a figure of merit (ZT) defined as $ZT = \frac{\sigma S^2}{\kappa_e + \kappa_L}T$ where σ, S, κ_e, κ_L, T are the electric conductivity, Seebeck coefficient, the electronic and lattice contribution to the total thermal conductivity, and temperature, respectively.[8] To achieve excellent TE performance, a high ZT value is needed. Thus, the material should both have a high power factor (PF), namely, σS^2, and a low thermal conductivity. However, this is not an easy task because these parameters are highly coupled.[9] Other novel approaches including nanostructure engineering,[10] band structure engineering,[11] defect introduction,[8] and increasing carrier mobility[12] have also been proved effective (Fig. 1).

TE materials have recently become a potential candidate for power supply in wearable devices. Inorganic TE materials have a key role. The most significant advantage of TE materials in this scenario is that it can harvest the heat dissipated by human bodies as a power source. According to the literature,[13] the power of heat generated by the human body can reach ~ 100 W. Even with a low-efficiency generator, such energy is still sufficient to drive some small devices like low-power microcontroller chips. However, traditional TE materials like selenides and tellurides are brittle inorganic semiconductors with poor flexibility.

Early approaches to wearable inorganic TE devices mainly involved unusual materials for TE like metal.[13] Other novel materials like carbon nanomaterials (*e.g.*, carbon nanotubes, graphene, carbon fibers, and fullerenes) and the carbon nano-material/conducting polymer composites are also possible candidates. Despite the ideal mechanical properties (flexibility) of

a Department of Physics, Southern University of Science and Technology, Shenzhen 518055, China. E-mail: huangs3@sustech.edu.cn, luy8@sustech.edu.cn, hejq@sustech.edu.cn

b Shenzhen Key Laboratory of Thermoelectric Materials, Southern University of Science and Technology, Shenzhen 518055, China

c Guangdong Provincial Key Laboratory of Energy Materials for Electric Power, Southern University of Science and Technology, Shenzhen 518055, China
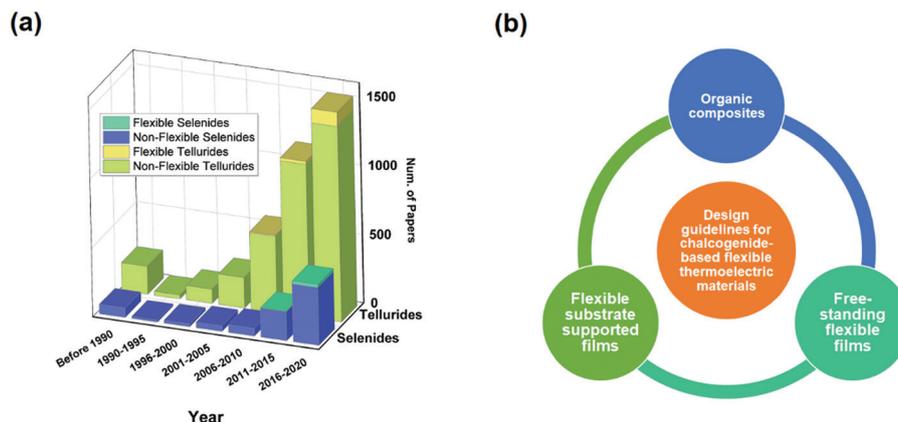
Fig. 1 (a) Research trend of telluride and selenide thermoelectric materials. Data retrieved from Web of Science with some tailored keywords, such as "selenide", "telluride", "flexible", and "thermoelectric". (b) Three design guidelines about the chalcogenide-based flexible thermoelectric materials and devices.

these materials, their thermoelectric performance is still poor. Another feasible approach is to make traditional bulk thermo-electric materials flexible. Most traditional TE material systems including chalcogenides (especially selenides and tellurides) have been widely studied since the 1950s. After decades of development, the physical properties of these materials have been thoroughly studied, and a possible means for performance enhancement has been proposed. Based on a large number of studies, people can take full advantage of the thermoelectric properties of these well-studied materials while finding ways to achieve flexibility and eventually apply them to wearable devices. Despite the short time of development (flexible chalcogenides were not reported until the 2000s), this approach has a key role in the field of flexible TE materials.

This review focuses on flexible TE materials, which mainly involve flexible chalcogenide-based films. Chalcogenide-based flexible thermoelectric materials have been discussed in three design guidelines: chalcogenides deposited on flexible films, organic-chalcogenide composites, and free-standing films. In each part, we first review the fabrication methods. The properties and performance of different materials are then discussed. A brief conclusion and outlook are also provided.

2. Strategies to realize flexible chalcogenide-based films

2.1 Chalcogenide-based films on a flexible substrate

To achieve high TE performance and good flexibility of thin films, one of the most commonly used methods is to deposit inorganic nanostructures on a flexible substrate. The common flexible substrates are polyimide (PI), polyether sulfone (PES),[14] and polyvinylidene fluoride (PVDF);[15,16] inorganic nanostructure-based films can maintain flexibility. The common fabrication processes are magnetron sputtering,[17–23] pulsed laser deposition,[24–26] thermal evaporation,[27,28] vacuum-assisted filtration and screen printing,[29,30] *etc.* Some additional methods like cold pressing and hot pressing[5,31] can maintain the comparable bulk-like ZT value through forming a

compacted film. However, the films are still rigid for wearable devices.

To make Cu_2Se flexible, Perez-Taborda *et al.*[32] deposited it on a PI substrate using pulsed reactive magnetron sputtering. The Cu_2Se film reached a high PF of 1100 μW m^{-1} K^{-2} at room temperature (RT). They[33] also used the same method to prepare Ag_2Se films, and a high PF of ~2440 μW m^{-1} K^{-2} at RT was obtained. However, due to the weak bonding strength between the inorganic and flexible substrates, it was difficult to form a highly flexible composite film.

Aside from magnetron sputtering, another solution to making Ag_2Se wearable—which itself is not flexible—is to use the hot pressing method for depositing the Ag_2Se nanowires on a flexible substrate like nylon membrane.[34,35] In 2019, Ding *et al.* developed a novel method to realize both high TE properties and excellent flexibility of the n-type Ag_2Se TE material.[34] They first prepared Ag_2Se nanowires using selenium nanowires as templates, and then used vacuum filtration to form a film on the nylon membrane. They finally hot pressed the material at 200 °C and 1 MPa for 30 min. A PF of 987.4 μW m^{-1} K^{-2} and a ZT value of ~0.6 were reached at RT. The film was also flexible and retained 80% of the electrical conductivity after 1500 bending cycles.

The high flexibility comes from the following three aspects. First, the substrate (nylon) is highly flexible. Furthermore, Ag_2Se nanowires after hot pressing form a web-like porous structure. Such a structure gives certain flexibility to the film.[36] There are also Ag and Se atoms that diffuse into the porous nylon membrane forming a strong bond between the film and substrate. Despite the excellent flexibility, the film still suffers from low PF *versus* Ag_2Se films on glass.[37] The main reason is that the growth orientation $(00l)$ does not agree with the orientation $(0l0)$ that has the highest PF.

Alternating the composition of the film can also have positive effects on TE properties. Lu *et al.* studied the influence of Cu addition on the TE properties of the Ag_2Se film and prepared a flexible n-type $Ag_2Se/Ag/CuAgSe$ film on the nylon membrane sub-strate (Fig. 2a).[35] The film reached a PF of 1593.9 μW m^{-1} K^{-2} at 300 K with a molar ratio of Cu : Ag : Se = 1 : 4 : 3.[35] It had superior
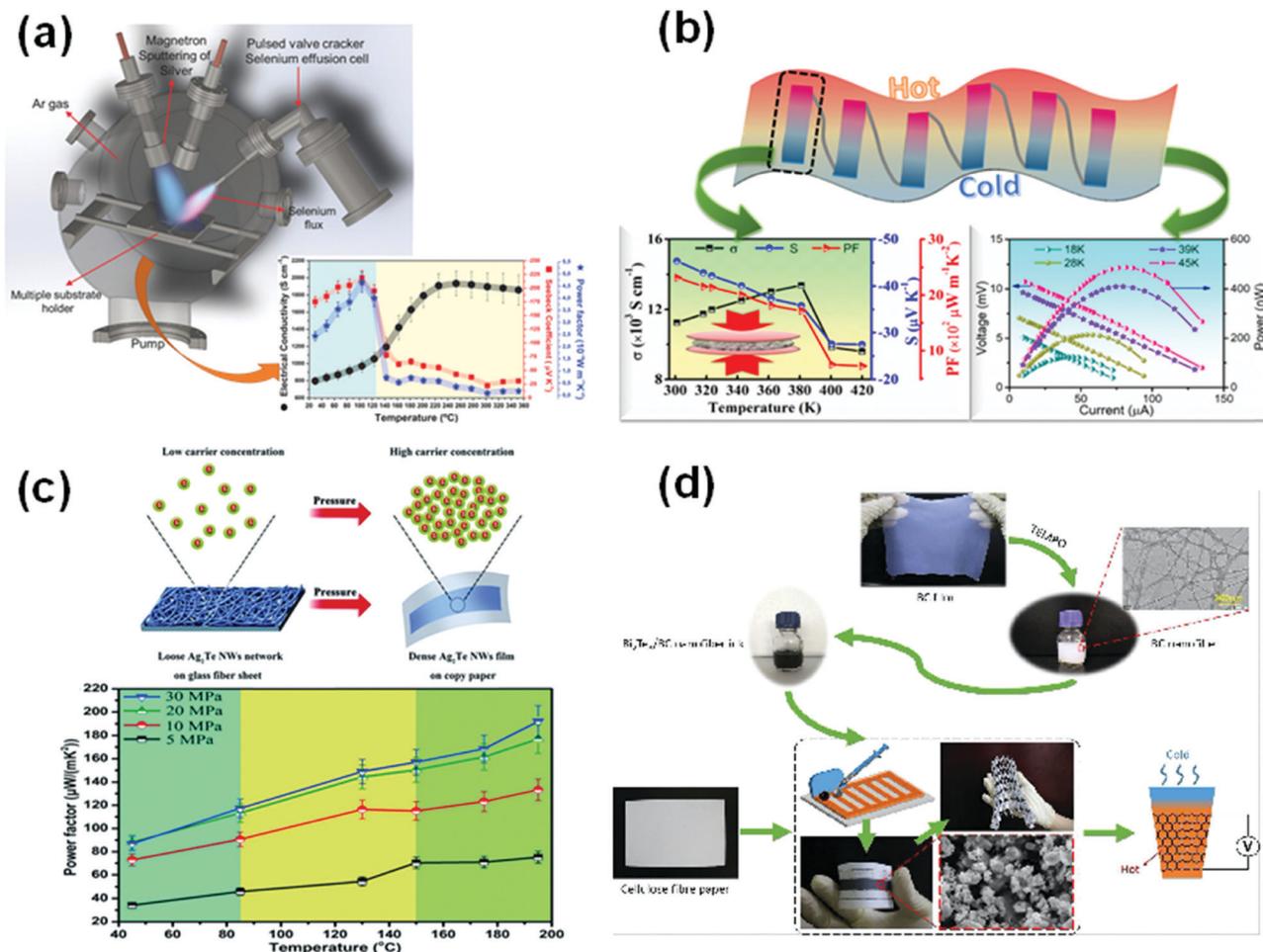
Fig. 2 (a) A cross-sectional diagram of the new method of manufacturing PHRMS deposition system is presented. The dependence on temperature for the Seebeck coefficient, electrical conductivity, and PF. (Reproduced and adapted with permission from ref. 33, copyright (2017) John Wiley & Sons.) (b) A highly flexible Ag_2Se-based composite film on nylon with a record PF is prepared for thermoelectric generator (reproduced with permission from ref. 35, copyright (2020) Royal Society of Chemistry). (c) A simulated diagram of carrier concentration and morphology of the Ag_2Te film before and after being compressed, and PF of the Ag_2Te film (reproduced with permission from ref. 47, copyright (2017) Royal Society of Chemistry). (d) Honeycomb-like TE generator based on paper (reproduced with permission from ref. 74, copyright (2019) Royal Society of Chemistry).

flexibility because the PF only dropped by 10% after 1000 bending cycles. The composition of the film was Ag nanoparticles, CuAgSe nanoparticles, and Ag_2Se nanograins. The electron conductivity is enhanced by Ag, which ejects electrons into the conduction band of the other two composites.[38] The energy filtering effect at the heterogeneous interfaces makes the composite film maintain a medium Seebeck coefficient. Furthermore, the defects in Ag_2Se grain and heterointerfaces of the composites scatter the short-wavelength phonons, which suppress the thermal conductivity of the film.[39] Besides, a flexible TEG is assembled using the optimum hybrid film, which generates a voltage and a maximum power density of 4.9 mV and 1.38 W m^{-2} at a temperature difference of 18 K. However, the enhancement of PF is mainly due to the greatly enhanced electrical conductivity. Hence, the corresponding electronic thermal conductivity is also high, leading to a lower ZT value ($ZT \sim 0.4$) at RT.

Jiang *et al.* studied Ag_2Se and tried to improve the processing procedure by suppressing the orientation of (00*l*) of the Ag_2Se

film and therefore enhancing the TE performance. A high PF of 1882 µW m^{-1} K^{-2} at RT was obtained.[40] They also assembled a flexible TEG, which created an output voltage of 4.3 mV under the 6.7 K temperature difference. By increasing the reaction temperature of Se nanowires and AgNO$_3$, Ag_2Se nanostructures are formed instead of Ag_2Se nanowires due to the reduction in surface energy. The formation of nanostructures suppresses the orientation of (00*l*), thus increasing the TE performance ($ZT \sim 0.8$ at RT).

Besides using the nylon membrane as the substrate, Gao *et al.* demonstrated a set of annealed paper-supported silver selenide films.[41] The PF of the $Ag_{2.3}Se$ film reached up to 2450.9 ± 364.4 µW m^{-1} K^{-2} at RT. An optimized length device was built using this film, which had an output power of 0.67 µW with a temperature difference of 25 K. Silver selenide showed tight bonding to the paper.

Besides Ag_2Se, other chalcogenides have also been proposed as possible candidates for flexible TE materials. Lin *et al.*

proposed a novel way to produce copper selenide films.[42] An ink solution of Cu_2Se was formed and deposited on the substrate *via* spin coating. Such a process secured a smooth and highly crystalline thin film (~ 55 nm), which was also void-free. Therefore, the high TE properties of copper selenides were secured. High flexibility was reached when the film is coated on a flexible substrate, *e.g.*, plastic.

In 2016, Yun *et al.* reported a mixture of HgSe and Ag nanoparticles deposited on flexible plastic films.[43] They confirmed that the electrical conductivity could be tuned by changing the ratio of Ag and HgSe NPs; an optimized *ZT* value and PF were reached. They presumed that such an optimization was achieved through adjustment of the carrier concentration. They further proposed that the energy barriers were lowered by Ag_2Se NPs attached to the surface of the HgSe NPs. The plastic film with NPs deposited showed high flexibility. The composite film showed a slight decrease in electric conductivity and an increase in the Seebeck coefficient.

By controlling the conditions of the reaction, Rongione *et al.* successfully synthesized SnSe nanosheets with a controlled growth direction.[44] The nanosheet has low thermal conductivity *versus* bulk SnSe. The boundary contributes most of the thermal resistivity because the thickness of the flakes is only about 150 nm. In other words, the thermal conductivity is suppressed, thus reaching a high TE performance. They also showed high flexibility by depositing the nanosheets on a polyethylene terephthalate substrate and performing bending tests. The thermal properties and electrical properties did not change much after 1000 cycles.

Attention has also been paid to the Ag_2Te nanostructure to see whether there is a possible way for flexible applications. The conducting type of Ag_2Te can be converted between n-type and p-type by adjusting the composition. In other words, excess Ag can act as an electron donor while superfluous Te can play a role as an electron acceptor.[45]

Finefrock *et al.*[46] synthesized Ag_2Te nanomaterials coated on a nylon fiber. After annealing the flexible film, the Seebeck coefficient changed from negative to positive, which indicated that Ag_2Te converted the conduction type from n-type to p-type. This is mainly due to the large changes in the stoichiometric ratio of Ag and Te before and after annealing. Compared with n-type Ag_2Te, the TE performance of the p-type one is much lower.[14,16] Therefore, mainstream research on the Ag_2Te TE material is n-type.

As for wearable devices application, the Ag_2Te-based films need to show competitive TE properties as well as good flexibility, *i.e.*, excellent durability. By introducing a novel glass fiber-auxiliary cold pressing method, Gao *et al.*[47] fabricated a Ag_2Te nanowire film supported on a copy-paper substrate that has a maximum PF of 192 μW m^{-1} K^{-2} at 468 K. The film showed good flexibility with a PF value decreasing by 20% after 500 bending cycles. However, its PF at RT is mediocre (88 μW m^{-1} K^{-2}) due to poor connection between Ag_2Te nanowires. To fix this problem, Zeng *et al.*[48] welded the Ag_2Te nanowires by vacuum filtration and drop-coating methods. The PF of the film is 152 μW m^{-1} K^{-2} at RT, which is almost twice as large as the film reported by Gao. The welding methods maintain the morphology of Ag_2Te nanowires,

which preserves low thermal conductivity. However, the flexibility is poor with electrical resistance increasing 30% after 1000 bending cycles.

Besides single component thermoelectric films, multiple component films have also shown their potential. Usually, Bi_2Te_3/Sb_2Te_3 thin films are not perfect candidates for flexible TE materials due to their deficient nanostructure, which can be—but are not limited to—poor interconnections and too many nanopores. Poor interconnection can result in the deduction of electrical conductivity and strain force concentration which makes thin films brittle.

To improve the interfacial bonding, Feng *et al.*[29] introduced Sb_2Te_3 as a nano-solder into Bi_2Te_3 films *via* screen-printing. The sample had excellent endurance and anti-oxidation (electric resistivity only changed by 3.6% after 6 months in the air). The porous structure of the film can withstand moderate deformation, which results in good flexibility and can effectively scatter the phonons. This special porous structure can reduce the thermal conductivity as well as the electrical conductivity.[49] Thus, efforts need to be made to find a moderate number of nanopores that can keep the balance of these parameters to optimize the flexible TE performance of materials. Jin *et al.*[50] used unbalanced magnetron sputtering technology to prepare Bi_2Te_3/cellulose fibers as flexible composites. Cellulose fibers have a porous structure, and the composite film can withstand deformation leading to high flexibility. The porous structure can also enhance phonon scattering, thus decreasing thermal conductivity. The PF values of the composite films are about 250–375 μW m^{-1} K^{-2} from RT to 473 K. The sample has a *ZT* value of 0.38 at 473 K.

The $(Bi, Sb)_2(Te, Se)_3$ TE bulk material has a high *ZT* value near RT, which is also a good candidate for flexible films. Researchers previously attempted to fabricate TE thin films by depositing $(Bi, Sb)_2(Te, Se)_3$ on different kinds of substrates (such as silica[27,51] and alumina[52,53]) using magnetron sputtering and screen printing processes.[54,55] However, the mechanical properties still cannot meet the requirements of flexible devices. Here, the flexibility of the TE thin film can be drastically improved by using organic substrates like polyimide (PI),[56–58] polyethylene terephthalate (PET),[59,60] and polycarbonate.[61] Nevertheless, the *ZT* value of the films is much lower than that of the bulks, because the poor crystallinity and texture on the substrate impede the enhancement of the *ZT* value. Furthermore, due to the thermolability of organic substrate, traditional annealing and sintering processes (>500 °C) cannot be employed on most organic substrates to improve the crystallinity and texture.[62,63] Thus, Danaei[64] *et al.* and Saeidi-Javash *et al.*[65] introduced a photonic sintering method into n-type $Bi_2Te_{2.7}Se_{0.3}$ to enhance its TE performance while maintaining flexibility. Although the PF of the n-type film that Saeidi-Javash *et al.* synthesized is not the highest $Bi_2Te_{2.7}Se_{0.3}$ film, the photonic sintering method can also dramatically reduce the synthesis time, which is beneficial to industrial mass production.[65]

The TE performance of p-type $Bi_{0.5}Sb_{1.5}Te_3$ bulk is higher than that of n-type $Bi_2Te_{2.7}Se_{0.3}$, and thus there are more studies on p-type systems. Like the n-type film, most studies

focused on adjusting the nanostructure of the film.[66] If the length of the porous structure is longer than the mean free path of electrons but shorter than that of phonons, then the high electrical conductivity can be maintained while simultaneously decreasing the thermal conductivity and thus improving the TE performance.[50,67] Kato et al.[68,69] introduced a porous structure using a block copolymer to reduce the thermal conductivity and obtain bulk-like ZT (about 1.34) for $Bi_{0.4}Sb_{1.6}Te_3$: this is an effective method to enhance the ZT value on a flexible thin film. However, the thermal conductivity is calculated by a model rather than an experiment; hence, the actual ZT value needs to be further confirmed. Besides, strengthening the connection of the interface can be another effective way to promote ZT value while also maintaining favorable flexibility.[29] Varghese et al.[70] added Te particles as nano-solders to successfully bridge the interface to $Bi_{0.4}Sb_{1.6}Te_3$ TE films by a screen printing method. Besides the extraordinary flexibility and endurance (electrical resistance only increases 3% after 1000 bending cycles with 10 mm radius), the printed films also exhibit the highest TE performance at RT: The PF is 3000 μW m^{-1} K^{-2} and ZT value is about 1, which demonstrates a significant leap for wearable TE applications.[70]

For the practical flexible TE devices, people usually combine the excellent performance of n-type $Bi_2Te_{2.7}Se_{0.3}$ and p-type $Bi_{0.5}Sb_{1.5}Te_3$ into flexible TEGs.[71–75] Meanwhile, due to the difficulty of measuring the thermal conductivity on thin films, the output power, power density, and other parameters of flexible TEGs become an important reference for the TE performance of materials.[76–78] Zhao et al.[74] introduced a honeycomb structure into the paper-based TEG fabricated by (Bi, Sb)$_2$(Te, Se)$_3$ and bacterial cellulose (Fig. 2b): this greatly improves the flexibility and water resistance and makes TEG applicable for a wide variety of surfaces. Feng et al.[79] prepared a flexible TEG through the combination with n-$Bi_2Te_{2.7}Se_{0.3}$ and p-$Bi_{0.5}Sb_{1.5}Te_3$ on PET film. The samples had an excellent output voltage (0.8 V) versus other flexible TEGs based on the same materials. Both flexible TEGs need about 50 K of a temperature difference to achieve a high power density, which is too large for wearable energy harvesting applications; however, this is acceptable for wearable temperature sensing[79] or wearable coolers.[80]

2.2 Organic-chalcogenide composites

Polymers possess an intrinsically low κ, which is independent of electrical optimization. Therefore, preparing organic/inorganic hybrids can be expected to combine the high PF of the inorganic filler and simultaneously low thermal conductivity of the polymer. Of the polymers, conducting polymers (CP) have an intrinsically high electrical conductivity. Suitable systems include poly(3,4-ethylenedioxythiophene) (PEDOT)[81] and poly(styrenesulfonate)-doped PEDOT (PEDOT:PSS)[46,82–85]—these can dramatically increase the flexibility of the chalcogenide-based composites. More importantly, some results show that TE performance improves due to the energy filtering effect of the organic/inorganic heterointerface.

For instance, Jao et al.[85] prepared Ag_2Te nanowires/PEDOT:PSS composites via physical mixing and developed a flexible TE nanogenerator. The nanogenerator showed a Seebeck coefficient

of 100 μV K^{-1}. However, because of the low efficiency, the nanogenerators were only aimed at temperature measurement in a multicomplex environment rather than wearable generators on the human body. Xu et al.[86] demonstrated the effectiveness of a dimensionality-morphology strategy on the improvement of flexible thermoelectric performance. They optimized the power density of (PVDF)/Ta_4SiTe_4 organic–inorganic composites to 13 W m^{-2} with a temperature difference of 35.5 K (Fig. 3a).

The organic solvent-assisted method can exfoliate inorganic compound nanosheets such as SnSe and Bi_2Te_3. Ju et al. combined tin selenide nanosheets with PEDOT:PSS.[87] First, a small amount of Te was added during the sintering process of the SnSe ingot. Then, $SnSe_{1-x}Te_x$ powders were intercalated by Li-ions, and $SnSe_{1-x}Te_x$ nanosheets were exfoliated from the powder. Finally, the nanosheets were combined with PEDOT:PSS through physical mixing, and a composite film was obtained by filtration. The introduction of trace Te during the sintering process can prepare an optimized hole concentration of the sample. The $SnSe_{0.97}Te_{0.03}$ nanosheet/PEDOT:PSS composite showed a PF of 14.7 μW m^{-1} K^{-2} with excellent durability after 1000 bending cycles. Du et al.[88] prepared Bi_2Te_3-based alloy nanosheets/PEDOT:PSS composites via exfoliation and drop-casting routes. The composite film containing 4.1 wt% Bi_2Te_3 showed higher electrical conductivity and a PF value of 32.3 μW m^{-1} K^{-2}.

In situ synthesis is an effective method to adequately disperse inorganic nanoparticles in a CP matrix, thus enhancing wettability and making the two phases robustly tethered. In 2016, Zaia et al. prepared controlled growth of PEDOT:PSS-coated Te–$Cu_{1.75}Te$ heterostructures using a facile solution-based synthesis method. They showed a creative synthetic method to grow nanoscale islands of $Cu_{1.75}Te$ alloy within hybrid PEDOT:PSS-Te nanowires. The PEDOT:PSS/Te/$Cu_{1.75}Te$ heterostructure nanocomposite was drop-cast on a glass substrate; this exhibited a 22% PF (84 μW m^{-1} K^{-2}) enhancement compared with PEDOT:PSS/Te. However, the film is not flexible. Lu et al.[89] prepared PEDOT:PSS-coated Te (PC-Te) nanorods in situ; PEDOT:PSS-coated polycrystal Cu_7Te_4 (PC-Cu_7Te_4) nanorods were then prepared using the PC-Te nanorods as templates. Finally, PC-Cu_7Te_4/PC-Te composite films were fabricated through physical mixing and drop-casting. The flexible ternary composite film showed an enhanced PF of 65.3 μW m^{-1} K^{-2} at 300 K, which is about five-fold as large as that of the PC-Cu_7Te_4 nanorod film and about three times as large as that of the PC-Te nanorod film.

The enhancement of the TE properties is ascribed to the synergetic effect of the two kinds of nanorods and the carrier filtering effect at the two heterointerfaces of Te/PEDOT:PSS and Cu_7Te_4/PEDOT:PSS. An eight single-leg flexible TEG consisting of the optimized composite film was fabricated: It produced a voltage of 31.2 mV and a maximum output power density of 0.395 W m^{-2} at a temperature gradient of 39 K (Fig. 3b). Inspired by the synthesis method of the PC-Cu_7Te_4 nanorod, they[90] synthesized PEDOT:PSS-coated Se (PC-Se) nanowires for the first time via an in situ chemical synthesis method. PEDOT:PSS-coated Cu_xSe_y (PC-Cu_xSe_y) nanowires were prepared by a template-directed synthesis method. Finally, PEDOT:PSS/Cu_xSe_y nanocomposite films on flexible nylon membranes were fabricated by vacuum-assisted
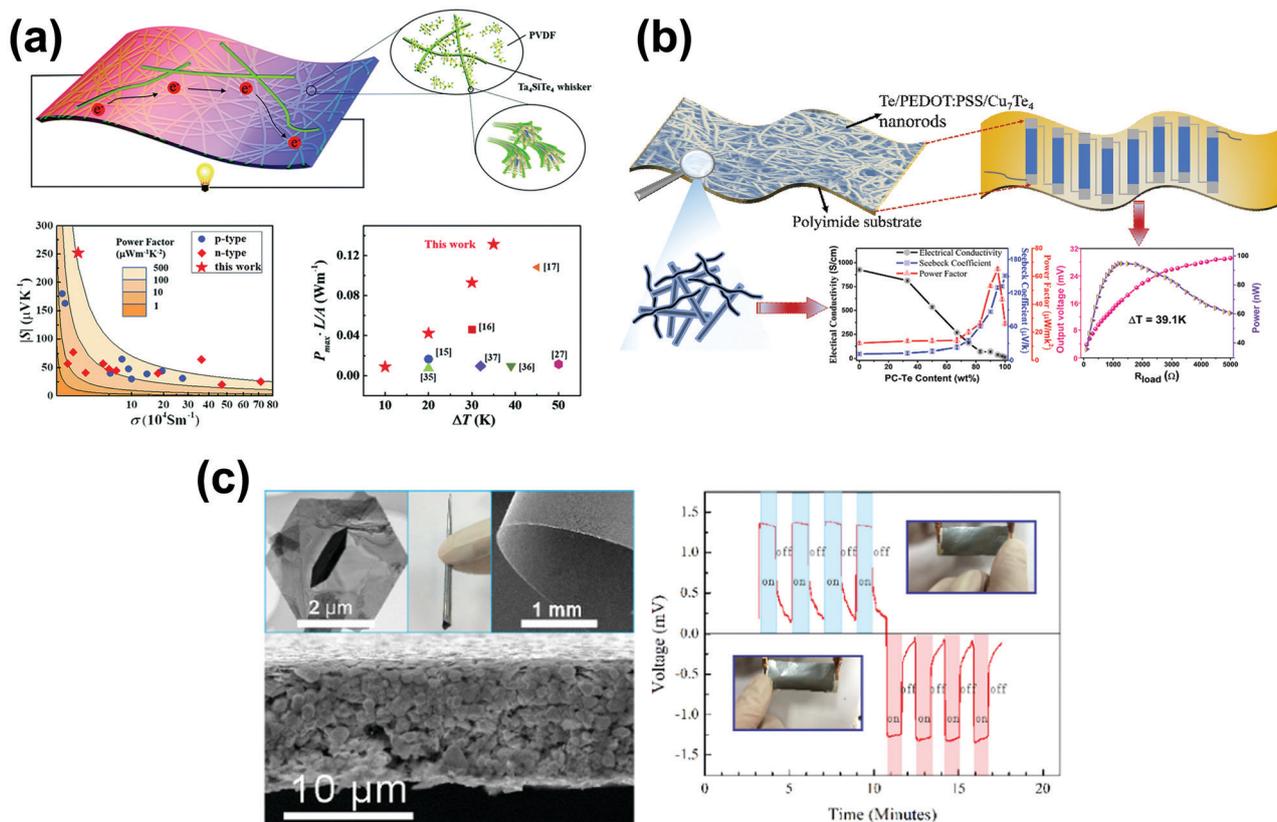
Fig. 3 (a) Synthesis and TE performance of the flexible PVDF/Ta$_4$SiTe$_4$ composite film (reproduced with permission from ref. 86, copyright (2020) Royal Society of Chemistry). (b) Performance of the flexible PC–Cu$_7$Te$_4$/PC–Te nanocomposite film and TE device (reproduced with permission from ref. 89, copyright (2018) American Chemical Society). (c) Flexible and freestanding n-type Cu$_{0.1}$Bi$_2$Se$_3$ nanoplatelet/PVDF TE composite film. Fingertip touch response of the Cu$_{0.1}$Bi$_2$Se$_3$ nanoplate based flexible thermoelectric films, which shows the thermoelectric films could continuously convert the body heat into electricity (reproduced with permission from ref. 94, copyright (2015) Elsevier.)

filtration and cold-pressing. An optimized PF $\sim$270.3 µW m^{-1} K^{-2} was obtained at 300 K.

The film exhibited superior flexibility with 83% of the original PF retention after bending for 1000 cycles around a rod with a diameter of 5 mm. Finally, a TE prototype composed of nine legs of the optimized hybrid film generated a voltage and a maximum power density of 15 mV and 0.91 W m^{-2}, respectively, at a temperature gradient of 30 K. To further improve the TE performance of the composite material, Cu^{2+} and Ag$^+$ were added to PC-Se nanowires in solution to perform a complete reaction. Then, an n-type PEDOT:PSS/Ag$_2$Se/CuAgSe composite film supported by porous nylon membrane was fabricated through vacuum-assisted filtration followed by hot-pressing. With PEDOT added, the RT thermal conductivity of the composite film remained low (0.458–0.800 W m^{-1} K^{-1}). As a result, the corresponding ZT value is $0.6 < ZT < 1.1$. After bending for 1000 cycles around a 4-mm radius rod, the PF decreases by only 8%. It showed excellent flexibility, which is attributed to the synergetic effect of the flexible nylon membrane and the porous PEDOT:PSS/Ag$_2$Se/CuAgSe composite film. Moreover, a flexible TE prototype composed of 11 single legs generated a voltage and a maximum power of 45.8 mV and 3.2 µW with a power density of 8.4 W m^{-2} at a temperature difference of 36 K.[91]

Most CP-based materials are p-type semiconductors and only generate positive TE power. To develop flexible n-type TE materials with negative TE power, researchers often use insulating polymers such as polyvinylidene fluoride (PVDF) and (polyvinylpyrrolidone) PVP to fabricate TE composites. Although the insulating polymer matrix can decrease the electrical conductivity of the composites, they also have some advantages over CPs, including lower cost, superior flexibility, and ultralow thermal conductivity.

Meng et al.[92] prepared an n-type PVP/Ag/Ag$_2$Te flexible composite film supported by a nylon filter membrane through vacuum-assisted filtration and heat treatment, where the PF is 217 µW m^{-1} K^{-2} and ZT is about 0.15–0.3 at 300 K. These show the highest TE performance among Ag$_2$Te-based composites. After 1000 rounds of bending tests, the electrical conductivity only decreased by 9.4%, which illustrates the excellent flexibility. A flexible TE device was assembled on a polyimide substrate using five n-type legs. The device has a maximum output power of 469 nW at a temperature difference of 39.6 K and a corresponding power density of 3.41 W m^{-2}.

PVDF can guarantee the robustness and flexibility of the composite film. In 2015, Dun et al.[93] reported a free-standing Bi$_2$Se$_3$ nanoplate/PVDF composite film through a drop-casting method. The PF is 30 µW m^{-1} K^{-2} at RT and dropped by 15%
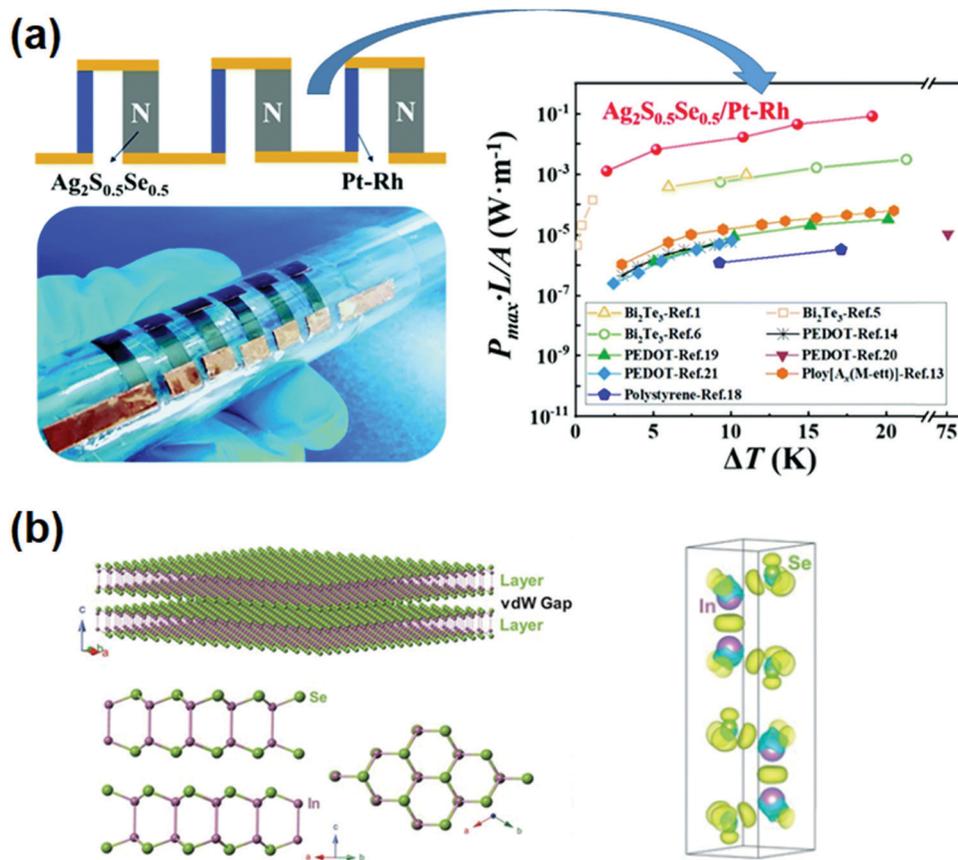
Fig. 4 (a) Six-couple flexible $Ag_2S_{0.5}Se_{0.5}$/Pt-Rh TE device and maximum power density (reproduced and adapted with permission from ref. 95, copyright (2019) Royal Society of Chemistry). (b) The InSe crystal structure and differential charge density (reproduced and adapted with permission from ref. 97, copyright (2020) American Association for the Advancement of Science).

after 1500 rounds of bending. They also prepared a freestanding n-type $Cu_{0.1}Bi_2Se_3$ nanoplatelet/PVDF TE composite film (Fig. 3c). The optimized PF and ZT of the composites are 103 μW m^{-1} K^{-2} and 0.1 at RT, respectively. They showed that PVDF can not only guarantee the flexibility but also introduce the energy barrier at the $Cu_{0.1}Bi_2Se_3$/PVDF heterointerface. Thus, high TE properties are maintained.[94]

2.3 Free-standing chalcogenide-based films

Organic substrates/components have poor stability at temperatures higher than 473 K, while free-standing inorganic flexible TE films can be applied at high temperatures. Liang et al.[95] reported high organic material-like flexibility and state-of-the-art ZT (up to 0.44 at 300 K and 0.63 at 450 K) in Ag_2S-based inorganic materials. Besides, a full-inorganic flexible TEG based on Ag_2(S, Se) and Ag_2(S, Te) was fabricated (Fig. 4a). The flexible full-inorganic device generated a high normalized maximum power density of 5.56 W m^{-2} under a temperature difference of 20 K. The discovery of intrinsic plastic deformability in bulk Ag_2S enabled fabrication of a fully inorganic Ag_2S-based flexible TEG.[96] More recently, Wei et al.[97] discovered exceptional deformability and plasticity in bulk single-crystalline InSe, which can be used in flexible TEG, sensors, photodetectors, etc. (Fig. 4b). Such extraordinary

mechanical properties stem from both the interlayer pliability and the interlayer long-range In–Se coulombic interaction across the van der Waals gap.

Besides flexible materials, changing the process conditions to alter the form of the product is also a feasible solution. Jin et al.[98] designed a creative new approach to produce high-performance TE materials using the SWCNT network as a scaffold to guide the deposition and growth of layer-structured Bi_2Te_3 nanocrystals to form a freestanding composite film. The ordered Bi_2Te_3/SWCNT interfaces can suppress the scattering of carriers during interfacial transport while dampening thermal conductivity due to porosity. The flexible films not only show excellent flexibility (bending radius <5 mm) but also exhibit high TE performance (bulk-like ZT value of 0.9 at RT).

3. Conclusion and outlook

In this review, we summarized recent progress on chalcogenide-based flexible TE films including organic/inorganic composites, inorganic films supported on flexible substrates, and full-inorganic films. Most bulk inorganic semiconductors are intrinsically brittle at ambient conditions. The high flexibility of the

traditional inorganic materials can be achieved by depositing nanostructures on the flexible substrates or combining them with flexible materials, *e.g.* PEDOT:PSS. For preparing inorganic films supported by flexible substrates, the power factor seems relatively high, and the flexibility is sometimes worse. For preparing organic/inorganic nanocomposite films, the TE property of inorganic material is higher than organic material, and it is important that the amount of the inorganic component is as high as possible, and because the two components have significantly different chemical properties, it is a great challenge to form a composite with perfect interfaces between the two phases. The discovery of intrinsic plastic deformability in bulk Ag_2S and InSe greatly promoted the development and application of all-inorganic flexible TE materials, which may be the focus of future research directions. Significant progress has been made toward developing these candidate materials with high TE performance and high flexibility.

Despite the promising performance given in the literature, the overall performance of flexible TE materials is still far from commercial application. Here, we give our outlook on future research:

1. To date, flexible TE films are mainly supported by flexible substrates. Since the desired device should be as small or as thin as possible, the substrate (which is often thicker than the film) should not use much space in the device. Therefore, a true free-standing flexible device should be the ultimate solution.

2. Since we have established an understanding of many other traditional bulk materials, endeavors should be made to apply these materials to flexible devices. Various approaches to boosting the TE performance of bulk thermoelectric materials have been proposed and can guide further enhancement of flexible TE materials.

3. Most papers mainly focus on increasing TE performance. However, the mechanical performance, *i.e.*, the origin of flexibility, has not yet been fully discussed or systematically explored. While many articles claimed that they have good flexibility, the damping of performance is still far from daily application. Thus, rediscovering the flexibility might be a new way to enhance the overall performance of flexible TE materials. Also, involving new geometrical architectures can bring several advantages.

4. The papers reviewed here rarely provided thermal properties; others provided the thermal conductivity of both the material and the film. These facts indicate a limitation of measuring methods. To fully understand the thermal properties, a new method for direct thermal conductivity measurement is needed.

With satisfying performances of wearable TEGs, it is predictable that many personal medical or sports devices will no longer need to charge a battery. Such new personal devices can remove worries about the power source and will increase convenience and quality of life.

Conflicts of interest

There are no conflicts to declare.

Acknowledgements

References

1 T. M. Tritt and M. A. Subramanian, *MRS Bull.*, 2006, **31**, 188–198.
2 E. D. M. Rowe, D. Ph, D. Sc and F. Group, *Thermoelectrics Handbook: Macro to Nano (Google eBook)*, 2010.
3 K. K. Jung, Y. Jung, C. J. Choi, J. M. Lee and J. S. Ko, *Curr. Appl. Phys.*, 2016, **16**, 1442–1448.
4 H. An, D. Karas, B. W. Kim, S. Trabia and J. Moon, *Nanotechnology*, 2018, **29**, 275403.
5 K. Ahmad and C. Wan, *Nanotechnology*, 2017, **28**, 415402.
6 S. B. Riffat and X. Ma, *Appl. Therm. Eng.*, 2003, **23**, 913–935.
7 B. Yang, H. Ahuja and T. N. Tran, *HVACR Res.*, 2008, **14**, 635–653.
8 L. Fu, M. Yin, D. Wu, W. Li, D. Feng, L. Huang and J. He, *Energy Environ. Sci.*, 2017, **10**, 2030–2040.
9 L. Fu, J. Cui, Y. Yu, Y. Huang, Y. Wang, Y. Chen and J. He, *J. Mater. Chem. A*, 2019, **7**, 6304–6311.
10 J. Zhang, D. Wu, D. He, D. Feng, M. Yin, X. Qin and J. He, *Adv. Mater.*, 2017, **29**, 1703148.
11 Y. Pei, X. Shi, A. Lalonde, H. Wang, L. Chen and G. J. Snyder, *Nature*, 2011, **473**, 66–69.
12 Y. Xiao, H. Wu, W. Li, M. Yin, Y. Pei, Y. Zhang, L. Fu, Y. Chen, S. J. Pennycook, L. Huang, J. He and L. D. Zhao, *J. Am. Chem. Soc.*, 2017, **139**, 18732–18738.
13 T. Starner, *IBM Syst. J.*, 1996, **35**, 618–629.
14 S. Yang, K. Cho, J. Yun, J. Choi and S. Kim, *Thin Solid Films*, 2017, **641**, 65–68.
15 C. Zhou, C. Dun, B. Ge, K. Wang, Z. Shi, G. Liu, D. L. Carroll and G. Qiao, *Nanoscale*, 2018, **10**, 14830–14834.
16 W. Wang, J. Liu, X. Li, Q. Jiang, J. Xu, C. Luo, P. Liu, R. Tan, Y. Du and F. Jiang, *J. Nanopart. Res.*, 2019, **21**, 131.
17 S. Liu, N. Peng, Y. Bai, D. Ma, F. Ma and K. Xu, *RSC Adv.*, 2016, **6**, 31668–31674.
18 T. Inamoto and M. Takashiri, *J. Appl. Phys.*, 2016, **120**, 1–8.
19 P. Nuthongkum, A. Sakulkalavek and R. Sakdanuphab, *J. Electron. Mater.*, 2017, **46**, 2900–2907.
20 P. Nuthongkum, R. Sakdanuphab, M. Horprathum and A. Sakulkalavek, *J. Electron. Mater.*, 2017, **46**, 6444–6450.

21 S. Kianwimol, P. Wanarattikan, R. Sakdanuphab, P. Pluengphon, T. Bovornratanaraks and A. Sakulkalavek, *J. Electron. Mater.*, 2019, **48**, 3490–3496.

22 K. Kusagaya, H. Hagino, S. Tanaka, K. Miyazaki and M. Takashiri, *J. Electron. Mater.*, 2015, **44**, 1632–1636.

23 K. Kusagaya and M. Takashiri, *J. Alloys Compd.*, 2015, **653**, 480–485.

24 E. Schwyter, W. Glatz, L. Durrer and C. Hierold, in 2008 Symposium on Design, Test, Integration and Packaging of MEMS/MOEMS, IEEE, 2008, pp. 46–48.

25 E. Koukharenko, X. Li, I. Nandhakumar, N. Frety, S. P. Beeby, D. Cox, M. J. Tudor, B. Schiedt, C. Trautmann, A. Bertsch and N. M. White, *J. Micromech. Microeng.*, 2008, **18**, 1–9.

26 W. Glatz, E. Schwyter, L. Durrer and C. Hierold, *J. Microelectromech. Syst.*, 2009, **18**, 763–772.

27 E. Symeou, C. Nicolaou, T. Kyratsi and J. Giapintzakis, *J. Appl. Phys.*, 2019, **125**, 0–9.

28 E. M. F. Vieira, J. Figueira, A. L. Pires, J. Grilo, M. F. Silva, A. M. Pereira and L. M. Goncalves, *J. Alloys Compd.*, 2019, **774**, 1102–1116.

29 J. Feng, W. Zhu, Y. Deng, Q. Song and Q. Zhang, *ACS Appl. Energy Mater.*, 2019, **2**, 2828–2836.

30 S. J. Kim, J. H. We and B. J. Cho, *Energy Environ. Sci.*, 2014, **7**, 1959–1965.

31 C. Dun, Y. Liu, A. Al-Qawasmeh, C. A. Hewitt, Y. Guo, J. Xu, Q. Jiang, J. Wang, G. Marcus, D. Cadavid, D. Montgomery, H. Wang, K. Kovnir, A. Cabot and D. L. Carroll, *2D Mater.*, 2018, **5**, 045008.

32 J. A. Perez-Taborda, L. Vera, O. Caballero-Calero, E. O. Lopez, J. J. Romero, D. G. Stroppa, F. Briones and M. Martin-Gonzalez, *Adv. Mater. Technol.*, 2017, **2**, 1700012.

33 J. A. Perez-Taborda, O. Caballero-Calero, L. Vera-Londono, F. Briones and M. Martin-Gonzalez, *Adv. Energy Mater.*, 2018, **8**, 1702024.

34 Y. Ding, Y. Qiu, K. Cai, Q. Yao, S. Chen, L. Chen and J. He, *Nat. Commun.*, 2019, **10**, 841.

35 Y. Lu, Y. Qiu, K. Cai, Y. Ding, M. Wang, C. Jiang, Q. Yao, C. Huang, L. Chen and J. He, *Energy Environ. Sci.*, 2020, **13**, 1240–1249.

36 W. Yang, S. Mao, J. Yang, T. Shang, H. Song, J. Mabon, W. Swiech, J. R. Vance, Z. Yue, S. J. Dillon, H. Xu and B. Xu, *Sci. Rep.*, 2016, **6**, 1–9.

37 J. A. Perez-Taborda, O. Caballero-Calero, L. Vera-Londono, F. Briones and M. Martin-Gonzalez, *Adv. Energy Mater.*, 2018, **8**, 1702024.

38 C. Dun, C. A. Hewitt, Q. Li, J. Xu, D. C. Schall, H. Lee, Q. Jiang and D. L. Carroll, *Adv. Mater.*, 2017, **29**, 1700070.

39 Y. Zhou, H. Wu, D. Wang, L. Fu, Y. Zhang, J. He, S. J. Pennycook and L. D. Zhao, *Mater. Today Phys.*, 2018, **7**, 77–88.

40 C. Jiang, Y. Ding, K. Cai, L. Tong, Y. Lu, W. Zhao and P. Wei, *ACS Appl. Mater. Interfaces*, 2020, **12**, 9646–9655.

41 J. Gao, L. Miao, H. Lai, S. Zhu, Y. Peng, X. Wang, K. Koumoto and H. Cai, *iScience*, 2020, **23**, 100753.

42 Z. Lin, C. Hollar, J. S. Kang, A. Yin, Y. Wang, H. Y. Shiu, Y. Huang, Y. Hu, Y. Zhang and X. Duan, *Adv. Mater.*, 2017, **29**, 1606662.

43 J. Yun, K. Cho, Y. Park, S. Yang, J. Choi and S. Kim, *Nano Res.*, 2017, **10**, 683–689.

44 N. A. Rongione, M. Li, H. Wu, H. D. Nguyen, J. S. Kang, B. Ouyang, H. Xia and Y. Hu, *Adv. Electron. Mater.*, 2019, **5**, 1800774.

45 P. F. Taylor and C. Wood, *J. Appl. Phys.*, 1961, **32**, 1–3.

46 S. W. Finefrock, X. Zhu, Y. Sun and Y. Wu, *Nanoscale*, 2015, **7**, 5598–5602.

47 J. Gao, L. Miao, C. Liu, X. Wang, Y. Peng, X. Wei, J. Zhou, Y. Chen, R. Hashimoto, T. Asaka and K. Koumoto, *J. Mater. Chem. A*, 2017, **5**, 24740–24748.

48 X. Zeng, L. Ren, J. Xie, D. Mao, M. Wang, X. Zeng, G. Du, R. Sun, J. B. Xu and C. P. Wong, *ACS Appl. Mater. Interfaces*, 2019, **11**, 37892–37900.

49 Z. Wu, E. Mu, Z. Che, Y. Liu, F. Sun, X. Wang and Z. Hu, *J. Alloys Compd.*, 2020, **828**, 154239.

50 Q. Jin, W. Shi, Y. Zhao, J. Qiao, J. Qiu, C. Sun, H. Lei, K. Tai and X. Jiang, *ACS Appl. Mater. Interfaces*, 2018, **10**, 1743–1751.

51 B. G. Kim, C. H. Lim, S. M. Choi, W. S. Seo, H. L. Lee, S. H. Hyun and S. M. Jeong, *CrystEngComm*, 2015, **17**, 7522–7527.

52 M. Kashiwagi, S. Hirata, K. Harada, Y. Zheng, K. Miyazaki, M. Yahiro and C. Adachi, *Appl. Phys. Lett.*, 2011, **98**, 023114.

53 S. J. Kim, H. Choi, Y. Kim, J. H. We, J. S. Shin, H. E. Lee, M. W. Oh, K. J. Lee and B. J. Cho, *Nano Energy*, 2017, **31**, 258–263.

54 J. Lee, H. Kim, L. Chen, S. H. Choi and V. K. Varadan, *Nanosyst. Eng. Med.*, 2012, **8548**, 85481C.

55 J. Lee, H. J. Kim, L. Chen, S. H. Choi, G. N. Mathur and V. K. Varadan, Nanosensors, Biosensors, Info-Tech Sensors Syst., 2013, **vol. 8691**, p. 86910R.

56 L. X. Liang, Y. Deng, Y. Wang, H. L. Gao and J. Cui, *J. Nanopart. Res.*, 2014, **16**, 1–7.

57 T. T. Shen and C. N. Liao, *Mater. Lett.*, 2017, **186**, 314–317.

58 E. Koukharenko, S. A. Boden, N. P. Sessions, N. Frety, I. Nandhakumar and N. M. White, *J. Mater. Sci.: Mater. Electron.*, 2018, **29**, 3423–3436.

59 S. H. Kim, T. Min, J. W. Choi, S. H. Baek, J. P. Choi and C. Aranas, *Energy*, 2018, **144**, 607–618.

60 R. Feng, F. Tang, N. Zhang and X. Wang, *ACS Appl. Mater. Interfaces*, 2019, **11**, 38616–38624.

61 A. Datta, A. Sangle, N. Hardingham, C. Cooper, M. Kraan, D. Ritchie, V. Narayan and S. Kar-Narayan, *Materials*, 2017, **10**, 553.

62 E. B. Secor, T. Z. Gao, M. H. Dos Santos, S. G. Wallace, K. W. Putz and M. C. Hersam, *ACS Appl. Mater. Interfaces*, 2017, **9**, 29418–29423.

63 E. B. Secor, B. Y. Ahn, T. Z. Gao, J. A. Lewis and M. C. Hersam, *Adv. Mater.*, 2015, **27**, 6683–6688.

64 R. Danaei, T. Varghese, M. Ahmadzadeh, J. McCloy, C. Hollar, M. Sadeq Saleh, J. Park, Y. Zhang and R. Panat, *Adv. Eng. Mater.*, 2018, **21**, 1800800.

65 M. Saeidi-Javash, W. Kuang, C. Dun and Y. Zhang, *Adv. Funct. Mater.*, 2019, **29**, 1901930.

66 P. Gao, L. Chen, B. Wu, Q. Zhang, C. Xue, C. Hou and Q. Sun, *J. Wuhan Univ. Technol., Mater. Sci. Ed.*, 2019, **34**, 781–786.

67 B. J. Last and D. J. Thouless, *Phys. Rev. Lett.*, 1971, **27**, 1719–1721.

68 K. Kato, Y. Hatasako, M. Kashiwagi, H. Hagino, C. Adachi and K. Miyazaki, *J. Electron. Mater.*, 2014, **43**, 1733–1739.

69 K. Kato, Y. Hatasako, M. Uchino, Y. Nakata, Y. Suzuki, T. Hayakawa, C. Adachi and K. Miyazaki, *Adv. Mater. Interfaces*, 2014, **1**, 1300015.

70 T. Varghese, C. Dun, N. Kempf, M. Saeidi-Javash, C. Karthik, J. Richardson, C. Hollar, D. Estrada and Y. Zhang, *Adv. Funct. Mater.*, 2020, **30**, 1905796.

71 G. Delaizir, J. Monnier, M. Soulier, R. Grodzki, B. Villeroy, J. Testard, J. Simon, C. Navone and C. Godart, *Sens. Actuators, A*, 2012, **174**, 115–122.

72 Z. Lu, M. Layani, X. Zhao, L. P. Tan, T. Sun, S. Fan, Q. Yan, S. Magdassi and H. H. Hng, *Small*, 2014, **10**, 3551–3554.

73 W. Zhu, Y. Deng, M. Gao and Y. Wang, *Energy Convers. Manage.*, 2015, **106**, 1192–1200.

74 X. Zhao, W. Han, Y. Jiang, C. Zhao, X. Ji, F. Kong, W. Xu and X. Zhang, *Nanoscale*, 2019, **11**, 17725–17735.

75 J. Luo, Z. Cao, M. Yuan and X. Chou, *Results Phys.*, 2019, **12**, 1304–1310.

76 B. Chen, M. Kruse, B. Xu, R. Tutika, W. Zheng, M. D. Bartlett, Y. Wu and J. C. Claussen, *Nanoscale*, 2019, **11**, 5222–5230.

77 J. Li, X. Tang, Y. Liu, Z. Yuan, Z. Xu and K. Liu, *Energy Technol.*, 2019, **7**, 1800707.

78 S. Kumar, H. H. Singh and N. Khare, *Energy Convers. Manage.*, 2019, **198**, 111783.

79 R. Feng, F. Tang, N. Zhang and X. Wang, *ACS Appl. Mater. Interfaces*, 2019, **11**, 38616–38624.

80 T. Zhang, K. Li, J. Zhang, M. Chen, Z. Wang, S. Ma, N. Zhang and L. Wei, *Nano Energy*, 2017, **41**, 35–42.

81 J. Na, Y. Kim, T. Park, C. Park and E. Kim, *ACS Appl. Mater. Interfaces*, 2016, **8**, 32392–32400.

82 E. J. Bae, Y. H. Kang, K. S. Jang, C. Lee and S. Y. Cho, *Nanoscale*, 2016, **8**, 10885–10890.

83 Y. Du, X. Liu, J. Xu and S. Z. Shen, *Mater. Chem. Front.*, 2019, **3**, 1328–1334.

84 Y.-C. Li and Z.-H. Lin, *ECS Trans.*, 2016, **72**, 67–71.

85 Y.-T. Jao, Y.-C. Li, Y. Xie and Z.-H. Lin, *ECS J. Solid State Sci. Technol.*, 2017, **6**, N3055–N3057.

86 Q. Xu, S. Qu, C. Ming, P. Qiu, Q. Yao, C. Zhu, T.-R. Wei, J. He, X. Shi and L. Chen, *Energy Environ. Sci.*, 2020, **13**, 511–518.

87 H. Ju, D. Park, K. Kim and J. Kim, *J. Alloys Compd.*, 2019, **792**, 638–643.

88 Y. Du, K. F. Cai, S. Chen, P. Cizek and T. Lin, *ACS Appl. Mater. Interfaces*, 2014, **6**, 5735–5743.

89 Y. Lu, Y. Qiu, Q. Jiang, K. Cai, Y. Du, H. Song, M. Gao, C. Huang, J. He and D. Hu, *ACS Appl. Mater. Interfaces*, 2018, **10**, 42310–42319.

90 Y. Lu, Y. Ding, Y. Qiu, K. Cai, Q. Yao, H. Song, L. Tong, J. He and L. Chen, *ACS Appl. Mater. Interfaces*, 2019, **11**, 12819–12829.

91 Y. Lu, Y. Qiu, K. Cai, X. Li, M. Gao, C. Jiang and J. He, *Mater. Today Phys.*, 2020, **14**, 100223.

92 Q. Meng, Y. Qiu, K. Cai, Y. Ding, M. Wang, H. Pu, Q. Yao, L. Chen and J. He, *ACS Appl. Mater. Interfaces*, 2019, **11**, 33254–33262.

93 C. Dun, C. A. Hewitt, H. Huang, J. Xu, D. S. Montgomery, W. Nie, Q. Jiang and D. L. Carroll, *ACS Appl. Mater. Interfaces*, 2015, **7**, 7054–7059.

94 C. Dun, C. A. Hewitt, H. Huang, J. Xu, C. Zhou, W. Huang, Y. Cui, W. Zhou, Q. Jiang and D. L. Carroll, *Nano Energy*, 2015, **18**, 306–314.

95 J. Liang, T. Wang, P. Qiu, S. Yang, C. Ming, H. Chen, Q. Song, K. Zhao, T. R. Wei, D. Ren, Y. Y. Sun, X. Shi, J. He and L. Chen, *Energy Environ. Sci.*, 2019, **12**, 2983–2990.

96 X. Shi, H. Chen, F. Hao, R. Liu, T. Wang, P. Qiu, U. Burkhardt, Y. Grin and L. Chen, *Nat. Mater.*, 2018, **17**, 421–426.

97 T. R. Wei, M. Jin, Y. Wang, H. Chen, Z. Gao, K. Zhao, P. Qiu, Z. Shan, J. Jiang, R. Li, L. Chen, J. He and X. Shi, *Science*, 2020, **369**, 542–545.

98 Q. Jin, S. Jiang, Y. Zhao, D. Wang, J. Qiu, D. M. Tang, J. Tan, D. M. Sun, P. X. Hou, X. Q. Chen, K. Tai, N. Gao, C. Liu, H. M. Cheng and X. Jiang, *Nat. Mater.*, 2019, **18**, 62–68.